

Article

Microbial-Based Biotechnology: Production and Evaluation of Selenium-Tellurium Nanoalloys

Arjun Muthu ^{1,2} , Daniella Sári ¹, Aya Ferroudj ¹, Hassan El-Ramady ^{1,3,*} , Áron Béni ², Khandsuren Badgar ^{4,*}  and József Prokisch ¹

- ¹ Nanofood Laboratory, Department of Animal Husbandry, Institute of Animal Science, Biotechnology and Nature Conservation, Faculty of Agricultural and Food Sciences and Environmental Management, University of Debrecen, 138 Böszörményi Street, 4032 Debrecen, Hungary; arjunvmuthu@gmail.com (A.M.); saridaniella91@gmail.com (D.S.); ferroudj.aya@agr.unideb.hu (A.F.); jprokisch@agr.unideb.hu (J.P.)
- ² Institute of Agricultural Chemistry and Soil Science, Faculty of Agricultural and Food Sciences and Environmental Management, University of Debrecen, 138 Böszörményi Street, 4032 Debrecen, Hungary; beniaro@agr.unideb.hu
- ³ Soil and Water Department, Faculty of Agriculture, Kafrelsheikh University, Kafr El-Sheikh 33516, Egypt
- ⁴ Department of Veterinary Basic Sciences, School of Veterinary Medicine, Mongolian University of Life Sciences, Zaisan, Khan-Uul District, Ulaanbaatar 17024, Mongolia
- * Correspondence: hassan.elramady@agr.kfs.edu.eg (H.E.-R.); b_khandsuren@mul.s.edu.mn (K.B.); Tel.: +976-88051094 (K.B.)

Abstract: Using seleno-compounds and telluric compounds is a practical approach for developing solutions against drug-resistant bacterial infections and malignancies. It will accelerate the search for novel treatments or adjuvants for existing therapies. Selenium and tellurium nanospheres can be produced by lactic acid bacteria. The bacteria can differentiate the selenium and tellurium when the medium contains both selenite and tellurite. Therefore, our question in this study was the following: are they making alloys from the selenium and tellurium and what will be the composition, color, and shape of the nanoparticles? We used a simple microbial synthesis to produce nanoselenium, nanotellurium, and their alloys from sodium selenite and sodium tellurite using *Lactobacillus casei*. This bacterium produced red spherical amorphous elemental selenium nanospheres with a diameter of 206 ± 33 nm from selenite and amorphous black nanorods with a length of 176 ± 32 nm and a cross-section of 62 ± 13 nm from tellurite. If the initial medium contains a mixture of selenite and tellurite, the resulting nanoparticles will contain selenium and tellurium in the same ratios in the alloy as in the medium. This proves that *Lactobacillus casei* cannot distinguish between selenite and tellurite. The shape of the nanoparticles varies from spherical to rod-shaped, depending on the ratio of selenium and tellurium. The color of nanomaterials ranges from red to black, depending on the percentage of selenium and tellurium. These nanomaterials could be good candidates in the pharmaceutical industry due to their antipathogenic and anticarcinogenic properties.

Keywords: green synthesis; *Lactobacillus casei*; nanoalloys; selenium; tellurium



Citation: Muthu, A.; Sári, D.; Ferroudj, A.; El-Ramady, H.; Béni, Á.; Badgar, K.; Prokisch, J. Microbial-Based Biotechnology: Production and Evaluation of Selenium-Tellurium Nanoalloys. *Appl. Sci.* **2023**, *13*, 11733. <https://doi.org/10.3390/app132111733>

Academic Editor: Ramona Iseppi

Received: 27 September 2023

Revised: 24 October 2023

Accepted: 25 October 2023

Published: 26 October 2023



Copyright: © 2023 by the authors. Licensee MDPI, Basel, Switzerland. This article is an open access article distributed under the terms and conditions of the Creative Commons Attribution (CC BY) license (<https://creativecommons.org/licenses/by/4.0/>).

1. Introduction

In the world, a huge risk to public health in the 21st century is multi-drug-resistant (MDR) bacterial infections [1] and MDR malignancies. More than 90% of deaths in cancer patients are due to drug resistance [2]. Unrestricted and unlicensed use of antibiotics has led to the rapid development of antibiotic resistance in bacterial strains [3]. O'Neill et al. predict that by 2050, MDR will put 10 million lives and \$100 trillion in total economic output at risk annually [4]. Therefore, developing new and effective anticancer and antibacterial agents is of great importance.

Nanotechnology involves creating materials at the atomic level that are stabilized by hydrophobic, electrostatic, coordinative, or hydrogen bonds. Stable nanoparticles (NPs)

can be generated in polymer solutions by reducing agents using several transformation methods. Volatile or toxic chemicals are commonly used for the synthesis of NPs. But recently, green synthesis of NPs and quantum dots (QDs) has become a trend due to their high bioavailability and low toxicity. NPs and QDs are popular as anticancer and antibacterial agents. QDs are small, spherical, light-emitting nanocrystalline particles. They are smaller than 10 nm and contain about 200 to 10,000 atoms. NPs can penetrate the bacterial cell wall and disrupt biochemical processes by disrupting organelles, ultimately destroying the bacterium [5].

Franz Josef Müller von Reichenstein discovered tellurium (Te) in 1783 in the Feis Banya mine in the Zartona region of Transylvania, Romania (formerly Hungary). There is an exciting story about the discovery of tellurium involving the famous music composer Wolfgang Amadeus Mozart. After 250 years, despite advances in nanotechnology, little research has been conducted on Te and tellurium nanoparticles (Te-NPs). Similar to other nanoparticle transformations, Te-NPs can be obtained using any conversion method. Generally, Te-NPs exhibit excellent anticancer and antibacterial properties. For example, ultrathin tellurium nanosheets combining photothermal effects and chemotherapy showed anticancer effects [6]. Also, aloe vera-mediated Te-NPs have shown anticancer activity against melanoma cells. This can be explained by damage to cellular proteins, lipids, nucleic acids, organelles, and membranes due to increased reactive oxygen species (ROS) levels [7].

Jöns Jacob Berzelius discovered selenium in a sample of pyrite in 1817 while producing sulfuric acid at the Falun mine in Stockholm, Sweden. Since then, many studies have been conducted on Se. NPs from selenium have presented many potential opportunities over the past 200 years. Se-NPs can also be prepared using other reductions such as γ -radiolysis, chemical, and biological reduction [8]. Actually, bacterial and plant metabolites mainly cause the biological transformation of NPs, strengthening and enhancing the reduction process, which is the most effective as it is cheap, rapid, and highly pure [9]. Se-NPs have several important characteristics including small size, atomic arrangement, shape, complex internal structure, and high surface area-to-volume ratio. Therefore, they can be used in a variety of applications including nanomedicine [10–12], food packaging [13,14], and food supplementation [15,16]. The size of Se-NPs determines their physical and biological properties. Smaller particle size always results in higher bioactivity. Their most important advantages are higher bioavailability and lower toxicity than organic and inorganic forms [17]. Se-NPs have been shown to have high antioxidant [18], detoxification [19,20], antibacterial [21,22], antifungal [23,24], antiviral [25], and antidiabetic effects [26]. For example, biosynthesized Se-NPs inhibited the growth of *Staphylococcus aureus* (*S. aureus*) [22,27], *Escherichia coli* (*E. coli*) [27], *Saccharomyces cerevisiae* (*S. cerevisiae*) [28], *Steinernema feltiae* (*S. feltiae*) [28], *Pseudomonas aeruginosa* (*P. aeruginosa*) [29], *Streptococcus pyogenes* (*S. pyogenes*) [27], and *Aspergillus clavatus* (*A. clavatus*) [27]. Also, they showed anticancer effects both in vitro [30] and in vivo [31] by inducing mitochondria-mediated apoptosis [32]. Actually, cancer cells are selenophilic and absorb selenium [33]. And Te has anticancer properties. Therefore, the combination of Se and Te would exhibit synergistic effects on MDR and cancer cells. If we could prove that cells cannot distinguish between Se and Te, the elements could be easily transported across membranes. As a preliminary study, we tested this hypothesis in bacterial cells.

This study included microbial synthesis of Se-NPs, Te-NPs, and selenium/tellurium nanoalloys (SeTe-NAs). We also tested whether bacteria were unable to distinguish between inorganic Te and Se in liquid culture.

2. Materials and Methods

Sodium selenite, sodium tellurite, MRS media, nitric acid 65% (AR grade), hydrogen peroxide, and hydrochloric acid 37% (AR grade) were obtained from VWR, International Ltd. (Lutterworth, Leics, UK). Sodium borohydride 98% (AR grade) was purchased from Acros Organics (Geel, Belgium). *Lactobacillus casei* (*L. casei*) NCAIM B 1147 was obtained from the National Collection of Agricultural and Industrial Microorganisms, Institute of

Food Science and Technology, Hungarian University of Agriculture and Life Sciences, Budapest, Hungary. Ultrapure water was used for all the experiments.

2.1. Sample Preparation

Samples were prepared with different concentrations of selenium and tellurium in 50 mL of sterile MRS (deMan, Rogosa, and Sharpe) broth containing stock solutions of sodium selenite and sodium tellurite, detailed in Table 1. All samples were incubated with a 2% *L. casei* inoculum suspension at 37 °C for 48 h. The samples were then centrifuged at 3000× *g* for 15 min to remove the supernatant. Then, the pellet was washed with ultrapure water and centrifuged at 3000× *g* for 15 min to remove contaminants.

Table 1. Selenium (Se) and tellurium (Te) concentrations in the MRS broth.

Sample	Se (mg dm ⁻³)	Te (mg dm ⁻³)	Se (nmol dm ⁻³)	Te (nmol dm ⁻³)	Se/(Se/Te) Molar Ratio in %
1.	100.3	0.0	1270	0.0	100
2.	100.3	0.0	1270	0.0	100
3.	100.1	0.3	1267	2.5	100
4.	99.9	0.7	1265	5.1	100
5.	99.3	1.6	1257	12.7	99
6.	98.3	3.3	1245	25.4	98
7.	96.3	6.5	1219	50.8	96
8.	94.3	9.8	1194	76.2	94
9.	92.3	13.0	1168	102	92
10.	90.3	16.3	1143	127	90
11.	75.2	40.6	953	318	75
12.	50.2	81.3	635	635	50
13.	25.1	121.9	318	953	25
14.	10.0	146.3	127	1143	10
15.	0.0	162.6	0	1270	0

2.2. Scanning Electron Microscopy and Energy-Dispersive X-ray Spectroscopy

The morphology and distribution of NPs were characterized by scanning electron microscopy (SEM) using a Hitachi S-4300-CFE (Tokyo, Japan) equipped with a field emission electron source. A Bruker (SDD) energy-dispersive X-ray detector was used to measure the elemental composition of the sample surface. NP samples were sequentially dehydrated in 50%, 60%, 70%, 80%, 90%, and 100% ethanol. Samples were dried on coverslips at room temperature before testing. For sample VII, optical microscopy and sectioning of the resin-embedded sample contained only tellurium.

2.3. Atomic Fluorescence Spectrophotometer

Se concentration was determined by measuring converted Te and Se from the pellet after centrifugation using an atomic fluorescence spectrophotometer (AFS) Millennium Excalibur 10.055 (PSA, Orpington, UK). Once the initial concentrations of Te and Se are known, the conversion efficiency can be calculated as a molar ratio. For sample preparation, 1 mL of the sample was mixed with 5 mL of nitric acid (65% *w/w*) at 60 °C for 3 h. Then, 3 mL of hydrogen peroxide (30% *w/w*) was added and further digested at 120 °C for 4 h. The sample was diluted with 3M hydrochloric acid and filtered through filter paper. Then, 3 mol L⁻¹ hydrochloric acid as a blank, 1.4% (*w/v*) sodium borohydride dissolved in 0.1 mol L⁻¹ sodium hydroxide as a reducing agent, and the sample were fed into the AFS instrument at a flow rate of 1 mL min⁻¹. Argon at 15 L min⁻¹ was used as drying gas. Analysis and storage times were kept at 25 and 30 s, respectively. All details on the preparing and measuring nanoalloy were inserted in Figure 1.



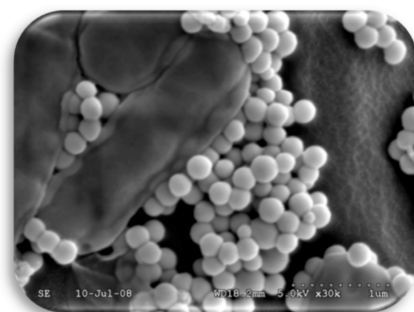
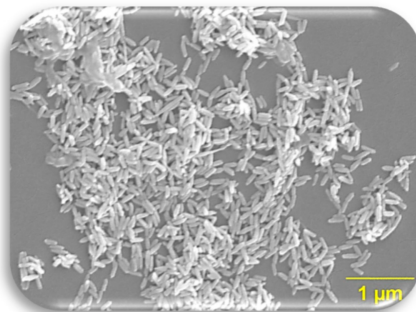
1. Selecting the tested bacteria species. Nano selenium formation by different bacteria in MRS media. The tested bacterium strains were: *Bifidobacterium lactis* BB-12; *Lactobacillus acidophilus* (LA-5); *Lactobacillus casei* NCAIM B 1147; and *Streptococcus thermophilus* in this experiment

2. Growing bacteria in milk + different concentrations of sodium selenite and sodium tellurite. Flasks contained mixed yogurt bacteria culture in milk (not MRS), where left flask is Te (200 mg L⁻¹), right is Se (200 mg L⁻¹), and mixtures between



3. Incubated with a 2% *L. casei* inoculum suspension at 37 °C for 48 h. Samples centrifuged at 3000× g for 15 min

4. The pellet was washed with ultrapure water and centrifuged at 3000× g for 15 min



5. Scanning nanoparticles using SEM for nano-Te

6. Scanning nanoparticles using SEM for nano-Se



7. Particle size analysis with a Malvern Mastersizer 2000

8. Millennium Excalibur atomic fluorescence spectrophotometer (AFS) to measure Se and Te

Figure 1. The main steps of the current study starting from selecting bacteria species to measuring the nano-content.

2.4. Statistical Analyses

All tests were run in triplicate and GraphPad Prism 9.5.0 was used to analyze the data. Linear and nonlinear regressions were evaluated at a significance level of $p \leq 0.05$. SEM images and particle size distributions were analyzed using ImageJ software (version 1.54 d, National Institutes of Health, Bethesda, MD, USA).

3. Results

3.1. Bacterial Synthesis of Se-NPs, Te-NPs, and SeTe-NAs

After inoculating activated *L. casei* NCAIM B 1147 into sodium selenite and sodium tellurite and incubating at 37 °C for 48 h, a time-dependent color change of the solution was observed (Figure 2). At the beginning of the reaction, the solution was clear and pale yellow. It later changed to light red (Se-NPs) and light black (Te-NPs). After 24 to 48 h of reaction, the color gradually changed to dark red and then black. After that, the red and black colors remained stable even with longer incubation times. The color of the SeTe-NAs depends on the concentration of selenite and tellurite present in it.



Figure 2. Samples containing only Se-NPs (tube no. 1), only Te-NPs (tube no. 15), and different combinations of the nanoalloy SeTe-NAs (tubes from 2 to 14) (from left to right). B refers to the control of Se or Te (without Se and Te) as the tube contains only MRS medium.

3.2. Morphological Characterization

The Se-NPs appeared spherical (Figure 3a), and the Te-NPs were rod-shaped (Figure 3b). SeTe-NAs were acicular with a poly-amorphous structure (Figure 3c) and were obviously heterogeneous in size. Prolonging the incubation period increased the number and size of these particles. The particle size distribution of Se-NPs shows that the diameter is 206 ± 33 nm. The Te-NP's diameter is 62 ± 13 nm and the length is 176 ± 32 nm. The diameter and length of SeTe-NPs are 74 ± 18 nm and 247 ± 33 nm, respectively. Figure 4a shows the peak at 1.4 keV confirming the presence of Se, while the peaks at 3.8 and 4.1 keV (Figure 4b) indicate a predominantly Te composition. Figure 4c includes peaks at 1.4, 3.8, and 4.1 keV, indicating the presence of Se and Te as alloys. The carbon (C) and gold (Au) peaks are correlated with the underlying coverslip.

The prepared samples were measured with an AFS instrument to determine the concentration present in both liquids and NPs. According to the experimental design, Se and Te were added such that the Se/(Se + Te) molar ratio tends to decrease throughout the sample. The Se/(Se + Te) molar ratio correlation remains unchanged regardless of the factors. A linear regression model (Figure 5) was constructed to establish the correlation between samples. Regression line $y = 0.9910X + 1.393$ with $R^2 = 0.9960$. The molar concentration ratio in the NPs is equal to the molar concentration ratio of the starting liquid medium. Bacteria converted inorganic Te and Se into elemental Te and Se [3,34,35]. Even SeTe-NPs are found in the same concentration molar ratio as those with inorganic Te and Se present in it. This indicates that the bacterial biotransformation efficiency of the initial selenite and tellurite concentrations remains constant.

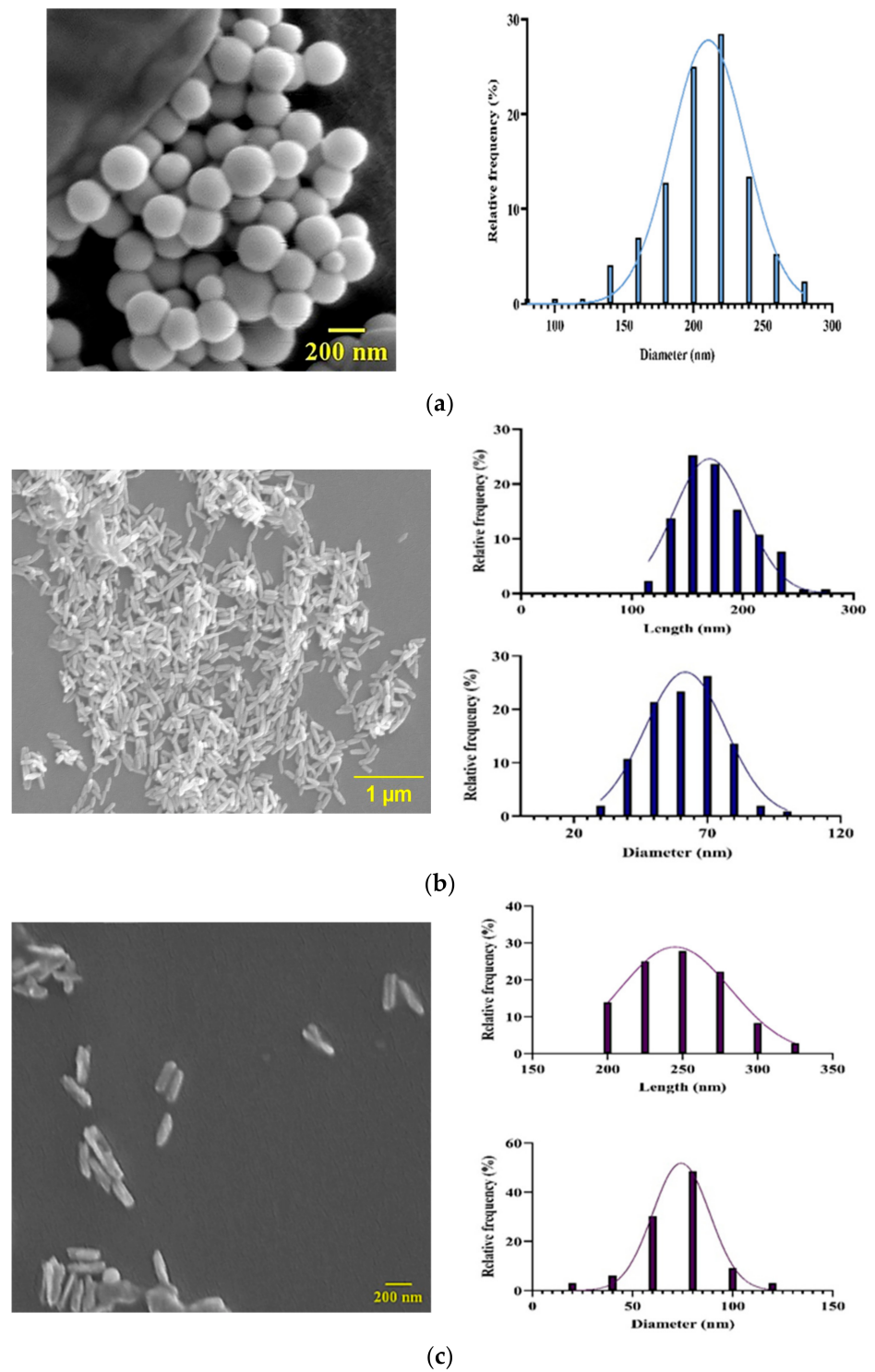


Figure 3. Particle size distribution and SEM images of (a) Se-NPs at 30,000 \times , (b) Te-NPs at 18,000 \times , and (c) SeTe-NAs at 25,000 \times magnification.

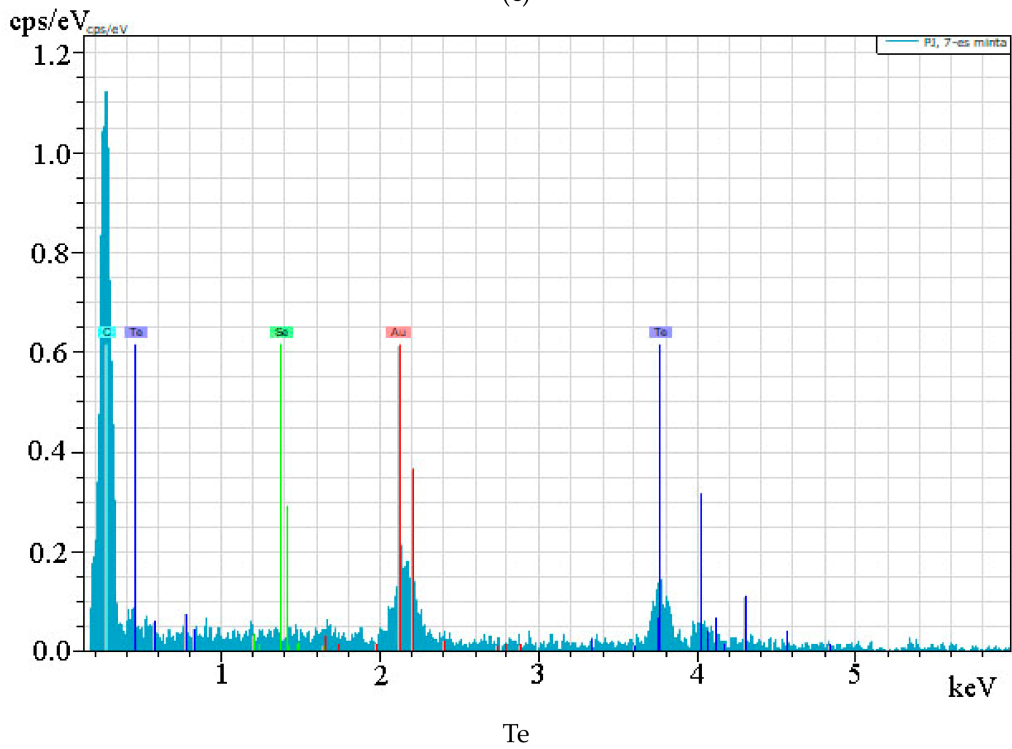
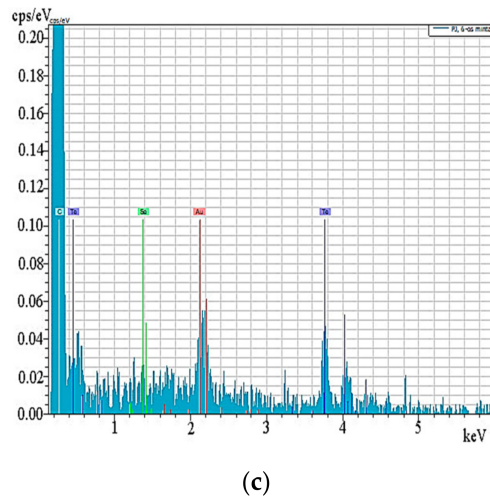
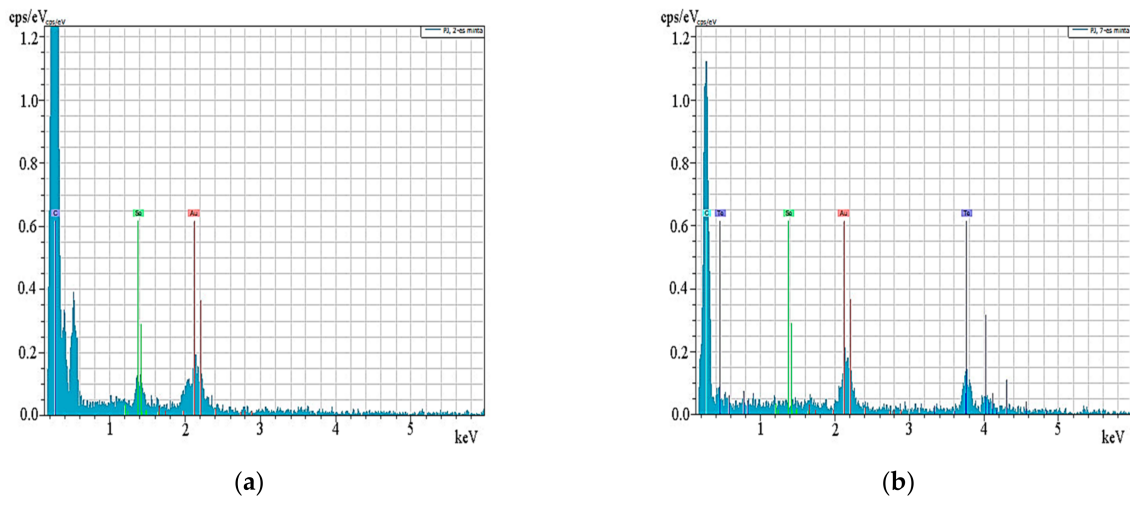


Figure 4. Cont.

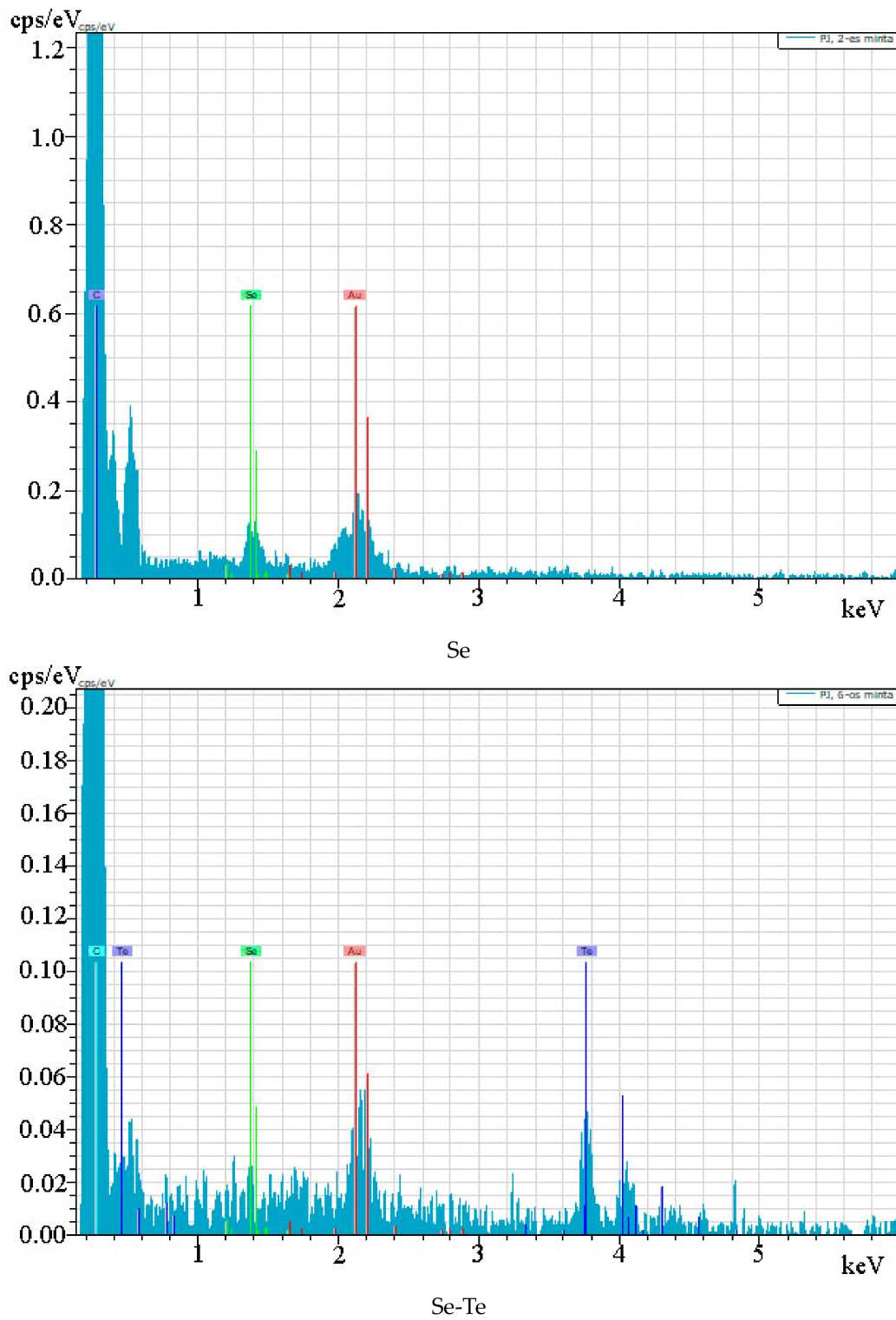


Figure 4. Energy dispersive spectra measured the elemental composition of the sample surface of (a) Se-NPs, (b) Te-NPs, and (c) SeTe-NAs.

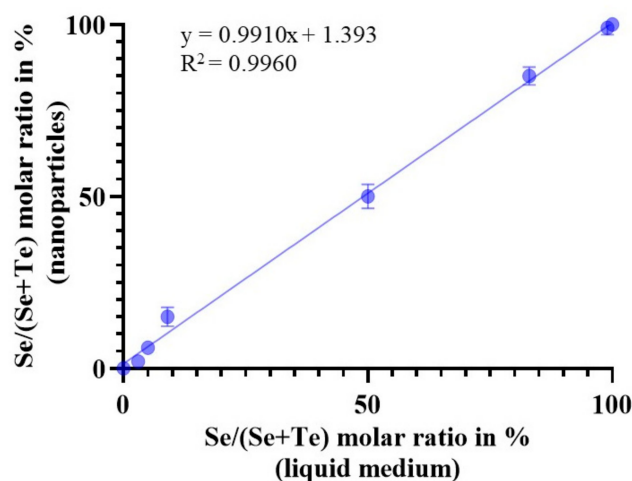


Figure 5. Se and Te molar ratio correlation between the samples ($p < 0.0001$).

4. Discussion

The main aim of our study is to produce a nanoalloy of Se and Te via the biological (microbial) method using bacterial species of *L. casei* NCAIM B 1147. This study opened several questions for our upcoming research on the production and application of Se and Te nanoalloys in medicine and other fields. The main questions that need to be answered are: Can the studied bacteria differentiate between nano-Se and/or nano-Te in their metabolism? To what extent are the studied bacteria tolerant to higher concentrations of Se and/or Te in bulk and in nanoform?

The monoclinic Se-NPs were red in color and had a glass transition temperature (T_g) of 31 °C [36]. Te-NPs are black in color, have a T_g of 37 °C [37], and can precipitate as an amorphous structure from solution at room temperature, exhibiting elemental Se and Te. The characteristic red and black colors of the solution were attributed to the surface plasmon vibrations and excitation of Se-NPs and Te-NPs [35]. The red color was mainly observed in samples with low concentrations of tellurite and high concentrations of selenite. The opposite phenomenon was observed for black samples. Se-NPs and Te-NPs with diameters of 221.1 nm and 76.1 nm were observed by Zonaro et al. [34]. Two types of morphology were discussed by Espinosa-Ortiz et al. [38]. The size of the acicular particles ranges from 50 to 600 nm, and the diameter of the sphere ranges from 70 to 300 nm, which correlates with this study.

We hypothesized that bacteria cannot distinguish between selenite and tellurite. Therefore, the concentration of SeTe-NAs remains the same as the Se/(Se + Te) molar ratio present in the initial medium. Bacteria may produce proton anti-transporters or reductases. Selenite and tellurite ions may react with these components to form nuclei of Se^0 and Te^0 . Subsequently, Se-NPs, Te-NPs, and SeTe-NAs are grown more significantly from these nuclei. Further conversion and aggregation of Se and Te atoms to Se and Te nuclei of selenite and tellurite ions involves an Ostwald ripening mechanism, in which small NPs form nuclei early in the growth stage. It acts as a formative seed and further grows through the maturation process [39].

Tellurium has a much stronger tendency to crystallize in the trigonal phase than selenium [40]. Te nanocrystals formed at the beginning of the synthesis can serve as heterogeneous seeds for the growth of Se and Te formed in the next step. Se and Te can form solids in solution and are isomorphic to each other. In random copolymers, Se and Te atoms are randomly arranged and distributed along the helical chain.

The conversion of tellurite to Te^0 and selenite to Se^0 depends on many factors, including the concentration of other ions other than oxyanions, pH, temperature, bacterial growth rate, and the nature of the medium. Previously, Se-NPs and Te-NPs have been shown to prevent biofilm and planktonic growth of *S. aureus* ATCC 25923, *P. aeruginosa* PAO1, and

E. coli JM109. They remove biofilms that have already formed and inhibit the formation of new biofilms. Compared to inorganic selenite, Se-NPs showed higher antimicrobial activity [34]. Se-NPs and Te-NPs obtained from *Ochrobactrum* sp. MPV1 and *Stenotrophomonas maltophilia* SeITE02 can induce ROS formation and inhibit microbial growth.

Te has the advantage of high optical absorption due to its chiral chain structure. It can be used for photodynamic therapy (PDT) and photothermal therapy (PTT) under single light source excitation. Modification of Te nanomaterials improves their biocompatibility, reduces toxicity, and confirms their therapeutic efficacy in biomedical applications [41]. Similarly, CdTe nanocrystals were obtained when *E. coli* cells were added to Na₂TeO₃ and CdCl₂ in a reducing environment. It has photoluminescence corresponding to its size with incubation time. The CdTe QDs had excellent crystallinity and consistent size. It was less toxic to eukaryotic cells when compared to hydrothermally synthesized particles. CdTe QDs can be used for cancer treatments due to their low toxicity [34].

Nanoparticle formation is usually considered as a defense mechanism against metal toxicity. The enhanced excretion or reduced absorption of the metals is their primary response to exposure to high metal concentrations. It includes either reductive precipitation or volatilization of selenite/tellurite [42,43]. A low degree of innate susceptibility to SeO₃²⁻/TeO₃²⁻ was exhibited by certain Gram-positive and Gram-negative bacteria [44,45]. Tellurite resistance has been established to be caused by chromosomal (Te^R) and plasmid-mediated tellurite resistance (Te^R) determinants [44].

Several enzymatic reductions by bacteria have been reported, such as thiol or glutathione reductase [46,47], sulphite reductase [48], fumarate reductase [49,50], Painter-type reaction [51], and nitrite reductase [52–54]. Depending on the bacterial type, the enzymatic reduction reaction can happen in the cytoplasm or periplasm [54]. Taylor et al. [55] explain that the TeO₃²⁻ enters the cell via the phosphate transporter. Nitrate reductases reduce it [52], where TeO₃²⁻ can be reduced to Te⁰. It can also be enzymatically converted to volatile hydride or methyl compounds via cellular-reduced thiols. Once selenite/tellurite enters the periplasm, it cannot be used as a distinctive electron acceptor. Reductase enzymes can reduce into Se⁰/Te⁰/SeTe-NAs [56].

Figure 6 explains the extracellular and intracellular formation of selenium. In the cytoplasm, Se⁰/Te⁰/SeTe-NAs formations are followed by the assembly of Se nanospheres/Te nanorods/SeTe-NAs poly-amorphous structures. Intracellular transport mechanisms are exhibited by cells to prevent accumulations of Se nanospheres/Te nanorods/SeTe-NAs [38,57]. *T. selenatis* transports the Se nanospheres out of the cell from the cytoplasm. Selenite is reduced to Se⁰ followed by the binding of SefA protein for assembling the Se nanosphere. It is lysed or transported outside the cell by an unknown mechanism [58,59]. Many unspecific proteins only interact with intracellular Se-NPs, resulting in excellent colloidal stability [60].

There is also an extracellular synthesis in the cytoplasm where selenite/tellurite is reduced to Se⁰/Te⁰/SeTe-NAs (Figure 7). It is followed by transportation across the membrane as a foreign entity outside the cell by an unknown export mechanism. Then, Se⁰/Te⁰/SeTe-NAs nuclei are assembled outside the cell into Se nanospheres/Te nanorods/SeTe-NAs poly-amorphous structures through an Ostwald-type ripening mechanism [39,40]. A similar possible mechanism has been reported by Sintubin et al. in silver nanoparticle synthesis [61]. Day by day, more concern is given to the green synthesis of Se- and Te-NPs, as reported by Zambonino et al. [62].

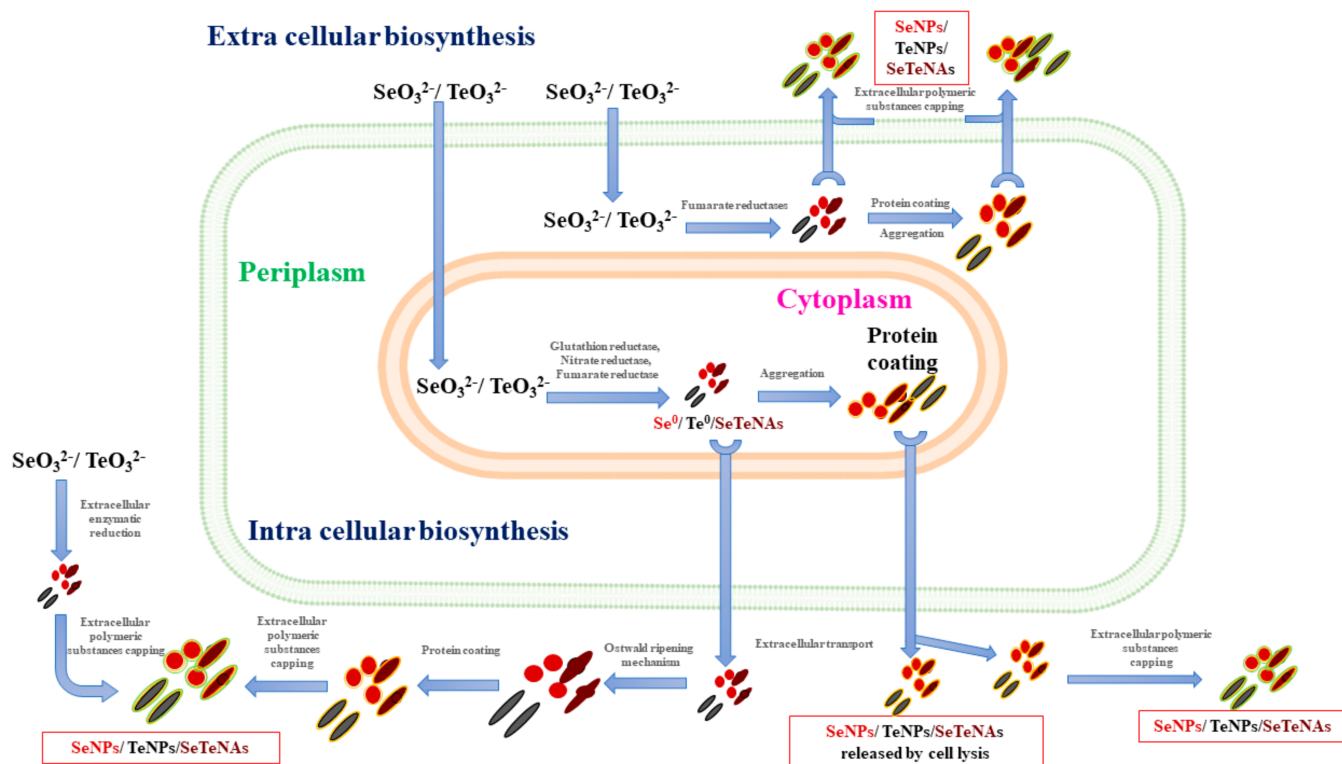


Figure 6. Proposed mechanism of selenite/tellurite reduction to Se-NPs/Te-NPs/SeTe-NAs.

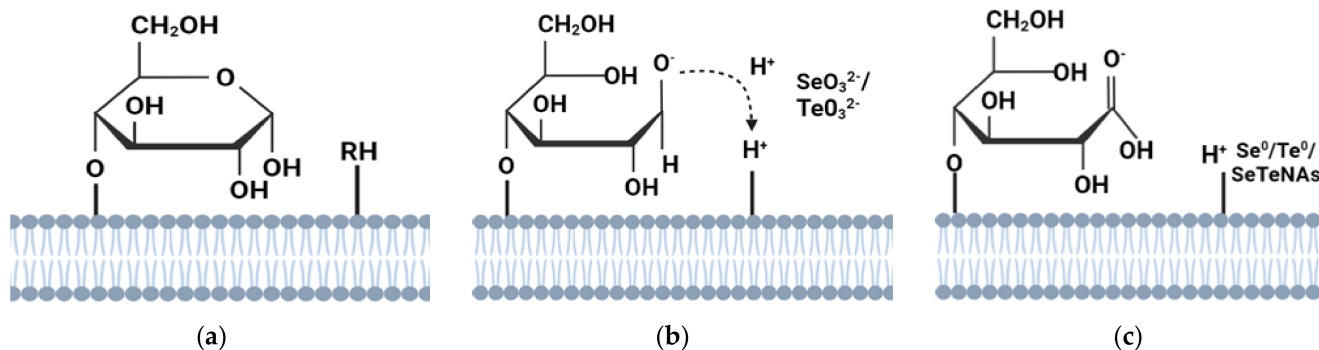


Figure 7. Suggested bacterial reduction of selenite/tellurite reduction to $\text{Se}^0/\text{Te}^0/\text{SeTe-NAs}$ at the cell surface. (a) Bacterial cell membrane with reducing sugars such as glucose and protonated anionic functional groups ($-\text{RH}$). (b) When pH increases, protons dissociate and create positively-charged adsorption sites for $\text{SeO}_3^{2-}/\text{TeO}_3^{2-}$. The open-ring structure of reducing sugars can reduce $\text{SeO}_3^{2-}/\text{TeO}_3^{2-}$ and (c) carboxylic acid is formed due to the oxidation of the aldehyde group of reducing sugar, while $\text{SeO}_3^{2-}/\text{TeO}_3^{2-}$ is reduced to $\text{Se}^0/\text{Te}^0/\text{SeTe-NAs}$.

5. Future Perspectives

The fabricated materials will be further evaluated for antimicrobial, anticancer, and other toxicity-related studies. This study strengthens the perspective of using Se-NPs, Te-NPs, and SeTe-NAs as potential antimicrobial agents. It can be effective and promising in cancer treatment in the future. There are still many further questions which need to be answered such as: What upcoming research is there on the nanoalloy of Se and Te? Is the produced nanoalloy of Se and Te important at the industrial medicine level? Which fields are promising? Are the produced nanoparticles antimicrobial towards another bacterium? To what extent are the produced alloy-nanoparticles toxic to *Lactobacilli* or other species? How do the *Lactobacilli* respond to the nanoparticles they secrete?

6. Conclusions

This study showed that *L. casei* NCAIM B 1147 can convert inorganic tellurite and selenite to Te^0 , Se^0 , and SeTe-NAs. We were able to demonstrate that bacterial cells cannot distinguish between selenite and tellurite. Regardless of the factors, Te and Se were transported into the cell and SeTe-NAs was synthesized. The molar concentration ratio $\text{Se}/(\text{Se} + \text{Te})$ of the generated NPs is equal to the $\text{Se}/(\text{Se} + \text{Te})$ molar ratio in the medium before inoculation. Therefore, cancer cells can absorb SeTe-NAs, and the synergistic effect of Se and Te is effective against pathogens and cancer cells. Bacterial synthesis is the most effective control and reduction process and is cheap, rapid, and highly pure. This environmentally friendly synthesis method of SeTe-NAs has great feasibility on a large scale for the pharmaceutical and therapeutic industries.

Author Contributions: Conceptualization, A.M., D.S., A.F., Á.B., K.B., H.E.-R. and J.P.; methodology, A.M., D.S., A.F., Á.B., K.B., H.E.-R. and J.P.; carried out the experiments, A.M., D.S. and A.F.; data analysis, A.M., D.S., A.F., Á.B., K.B., H.E.-R. and J.P.; writing—original draft preparation, K.B., H.E.-R. and J.P. All authors have read and agreed to the published version of the manuscript.

Funding: The research was funded by the Stipendium Hungaricum Scholarship Program.

Institutional Review Board Statement: Not applicable.

Informed Consent Statement: Not applicable.

Data Availability Statement: The data presented in this study are available on request from the corresponding author.

Acknowledgments: The authors thank Lajos Daróczy, Solid State Physics Department, University of Debrecen, for SEM analysis.

Conflicts of Interest: The authors declare no conflict of interest.

References

1. World Health Organization. Antimicrobial Resistance: Global Report on Surveillance 2014—World, ReliefWeb. Available online: <https://reliefweb.int/report/world/antimicrobial-resistance-global-report-surveillance-2014> (accessed on 11 September 2023).
2. Bukowski, K.; Kciuk, M.; Kontek, R. Mechanisms of Multidrug Resistance in Cancer Chemotherapy. *Int. J. Mol. Sci.* **2020**, *21*, 3233. [[CrossRef](#)] [[PubMed](#)]
3. Singh, A.; Gautam, P.K.; Verma, A.; Singh, V.; Shivapriya, P.M.; Shivalkar, S.; Sahoo, A.K.; Samanta, S.K. Green Synthesis of Metallic Nanoparticles as Effective Alternatives to Treat Antibiotics Resistant Bacterial Infections: A Review. *Biotechnol. Rep. Amst. Neth.* **2020**, *25*, e00427. [[CrossRef](#)] [[PubMed](#)]
4. O'Neill, J. *Tackling Drug-Resistant Infections Globally: Final Report and Recommendations*; Government of the United Kingdom: London, UK, 2016.
5. Arakha, M.; Pal, S.; Samantarrai, D.; Panigrahi, T.K.; Mallick, B.C.; Pramanik, K.; Mallick, B.; Jha, S. Antimicrobial Activity of Iron Oxide Nanoparticle upon Modulation of Nanoparticle-Bacteria Interface. *Sci. Rep.* **2015**, *5*, 14813. [[CrossRef](#)] [[PubMed](#)]
6. Pan, W.; Liu, C.; Li, Y.; Yang, Y.; Li, W.; Feng, C.; Li, L. Ultrathin Tellurium Nanosheets for Simultaneous Cancer Thermo-Chemotherapy. *Bioact. Mater.* **2022**, *13*, 96–104. [[CrossRef](#)]
7. Longa, P. A Háromszor Felfedezett Tellúr Avagy Geológusok a Varázsfuvolában—PDF Free Download. Available online: <https://docplayer.hu/1876368-A-haromszor-felfedezett-tellur-avagy-geologusok-a-varazsfuvolaban.html> (accessed on 11 September 2023).
8. Badgar, K. The Synthesis of Selenium Nanoparticle (SeNPs)—Review. *Acta Agrar. Debreceniensis* **2019**, *1*, 5–8. [[CrossRef](#)]
9. Khandsuren, B.; Prokisch, J. The Production Methods of Selenium Nanoparticles. *Acta Univ. Sapientiae Aliment.* **2021**, *14*, 14–43. [[CrossRef](#)]
10. Hosnedlova, B.; Kepinska, M.; Skalickova, S.; Fernandez, C.; Ruttkay-Nedecky, B.; Peng, Q.; Baron, M.; Melcova, M.; Opatrilova, R.; Zidkova, J.; et al. Nano-Selenium and Its Nanomedicine Applications: A Critical Review. *Int. J. Nanomed.* **2018**, *13*, 2107–2128. [[CrossRef](#)]
11. Zhang, J.; Zhou, X.; Yu, Q.; Yang, L.; Sun, D.; Zhou, Y.; Liu, J. Epigallocatechin-3-Gallate (EGCG)-Stabilized Selenium Nanoparticles Coated with Tet-1 Peptide to Reduce Amyloid- β Aggregation and Cytotoxicity. *ACS Appl. Mater. Interfaces* **2014**, *6*, 8475–8487. [[CrossRef](#)]
12. Kheradmand, E.; Rafii, F.; Yazdi, M.H.; Sepahi, A.A.; Shahverdi, A.R.; Oveisi, M.R. The Antimicrobial Effects of Selenium Nanoparticle-Enriched Probiotics and Their Fermented Broth against *Candida albicans*. *DARU J. Pharm. Sci.* **2014**, *22*, 48. [[CrossRef](#)]

13. Vera, P.; Canellas, E.; Nerín, C. New Antioxidant Multilayer Packaging with Nanoselenium to Enhance the Shelf-Life of Market Food Products. *Nanomaterials* **2018**, *8*, 837. [[CrossRef](#)]
14. Vera, P.; Echegoyen, Y.; Canellas, E.; Nerín, C.; Palomo, M.; Madrid, Y.; Cámara, C. Nano Selenium as Antioxidant Agent in a Multilayer Food Packaging Material. *Anal. Bioanal. Chem.* **2016**, *408*, 6659–6670. [[CrossRef](#)] [[PubMed](#)]
15. Skalickova, S.; Milosavljevic, V.; Cihalova, K.; Horky, P.; Richtera, L.; Adam, V. Selenium Nanoparticles as a Nutritional Supplement. *Nutrition* **2017**, *33*, 83–90. [[CrossRef](#)] [[PubMed](#)]
16. Garousi, F. The Essentiality of Selenium for Humans, Animals, and Plants, and the Role of Selenium in Plant Metabolism and Physiology. *Acta Univ. Sapientiae Aliment.* **2017**, *10*, 75–90. [[CrossRef](#)]
17. Ungvári, É.; Monori, I.; Megyeri, A.; Csiki, Z.; Prokisch, J.; Sztrik, A.; Jávora, A.; Benkő, I. Protective Effects of Meat from Lambs on Selenium Nanoparticle Supplemented Diet in a Mouse Model of Polycyclic Aromatic Hydrocarbon-Induced Immunotoxicity. *Food Chem. Toxicol.* **2014**, *64*, 298–306. [[CrossRef](#)] [[PubMed](#)]
18. Wang, H.; Zhang, J.; Yu, H. Elemental Selenium at Nano Size Possesses Lower Toxicity without Compromising the Fundamental Effect on Selenoenzymes: Comparison with Selenomethionine in Mice. *Free Radic. Biol. Med.* **2007**, *42*, 1524–1533. [[CrossRef](#)] [[PubMed](#)]
19. Trabelsi, H.; Azzouz, I.; Ferchichi, S.; Tebourbi, O.; Sakly, M.; Abdelmelek, H. Nanotoxicological Evaluation of Oxidative Responses in Rat Nephrocytes Induced by Cadmium. *Int. J. Nanomed.* **2013**, *8*, 3447–3453. [[CrossRef](#)] [[PubMed](#)]
20. Prasad, K.S.; Selvaraj, K. Biogenic Synthesis of Selenium Nanoparticles and Their Effect on As(III)-Induced Toxicity on Human Lymphocytes. *Biol. Trace Elem. Res.* **2014**, *157*, 275–283. [[CrossRef](#)]
21. Fardsadegh, B.; Vaghari, H.; Mohammad-Jafari, R.; Najian, Y.; Jafarizadeh-Malmiri, H. Biosynthesis, Characterization and Antimicrobial Activities Assessment of Fabricated Selenium Nanoparticles Using Pelargonium Zonale Leaf Extract. *Green Process. Synth.* **2019**, *8*, 191–198. [[CrossRef](#)]
22. Shoeibi, S.; Mashreghi, M. Biosynthesis of Selenium Nanoparticles Using Enterococcus Faecalis and Evaluation of Their Antibacterial Activities. *J. Trace Elem. Med. Biol.* **2017**, *39*, 135–139. [[CrossRef](#)]
23. Gunti, L.; Dass, R.S.; Kalagatur, N.K. Phytofabrication of Selenium Nanoparticles From Emblica Officinalis Fruit Extract and Exploring Its Biopotential Applications: Antioxidant, Antimicrobial, and Biocompatibility. *Front. Microbiol.* **2019**, *10*, 931. [[CrossRef](#)]
24. Fardsadegh, B.; Jafarizadeh-Malmiri, H. Aloe Vera Leaf Extract Mediated Green Synthesis of Selenium Nanoparticles and Assessment of Their In Vitro Antimicrobial Activity against Spoilage Fungi and Pathogenic Bacteria Strains. *Green Process. Synth.* **2019**, *8*, 399–407. [[CrossRef](#)]
25. Ramya, S.; Shanmugasundaram, T.; Balagurunathan, R. Biomedical Potential of Actinobacterially Synthesized Selenium Nanoparticles with Special Reference to Anti-Biofilm, Anti-Oxidant, Wound Healing, Cytotoxic and Anti-Viral Activities. *J. Trace Elem. Med. Biol.* **2015**, *32*, 30–39. [[CrossRef](#)] [[PubMed](#)]
26. Zhao, S.-J.; Wang, D.-H.; Li, Y.-W.; Han, L.; Xiao, X.; Ma, M.; Wan, D.C.-C.; Hong, A.; Ma, Y. A Novel Selective VPAC2 Agonist Peptide-Conjugated Chitosan Modified Selenium Nanoparticles with Enhanced Anti-Type 2 Diabetes Synergy Effects. *Int. J. Nanomed.* **2017**, *12*, 2143–2160. [[CrossRef](#)]
27. Srivastava, N.; Mukhopadhyay, M. Green Synthesis and Structural Characterization of Selenium Nanoparticles and Assessment of Their Antimicrobial Property. *Bioprocess Biosyst. Eng.* **2015**, *38*, 1723–1730. [[CrossRef](#)] [[PubMed](#)]
28. Estevam, E.C.; Griffin, S.; Nasim, M.J.; Denezhkin, P.; Schneider, R.; Lilischkis, R.; Dominguez-Alvarez, E.; Witek, K.; Latacz, G.; Keck, C.; et al. Natural Selenium Particles from *Staphylococcus carnosus*: Hazards or Particles with Particular Promise? *J. Hazard. Mater.* **2017**, *324*, 22–30. [[CrossRef](#)] [[PubMed](#)]
29. Cremonini, E.; Zonaro, E.; Donini, M.; Lampis, S.; Boaretti, M.; Dusi, S.; Melotti, P.; Lleo, M.M.; Vallini, G. Biogenic Selenium Nanoparticles: Characterization, Antimicrobial Activity and Effects on Human Dendritic Cells and Fibroblasts. *Microb. Biotechnol.* **2016**, *9*, 758–771. [[CrossRef](#)] [[PubMed](#)]
30. Ramamurthy, C.H.; Sampath, K.S.; Arunkumar, P.; Kumar, M.S.; Sujatha, V.; Premkumar, K.; Thirunavukkarasu, C. Green Synthesis and Characterization of Selenium Nanoparticles and Its Augmented Cytotoxicity with Doxorubicin on Cancer Cells. *Bioprocess Biosyst. Eng.* **2013**, *36*, 1131–1139. [[CrossRef](#)] [[PubMed](#)]
31. Yazdi, M.H.; Mahdavi, M.; Varastehmoradi, B.; Faramarzi, M.A.; Shahverdi, A.R. The Immunostimulatory Effect of Biogenic Selenium Nanoparticles on the 4T1 Breast Cancer Model: An In Vivo Study. *Biol. Trace Elem. Res.* **2012**, *149*, 22–28. [[CrossRef](#)]
32. Chen, T.; Wong, Y.-S.; Zheng, W.; Bai, Y.; Huang, L. Selenium Nanoparticles Fabricated in Undaria Pinnatifida Polysaccharide Solutions Induce Mitochondria-Mediated Apoptosis in A375 Human Melanoma Cells. *Colloids Surf. B Biointerfaces* **2008**, *67*, 26–31. [[CrossRef](#)]
33. Carlisle, A.E.; Lee, N.; Matthew-Onabanjo, A.N.; Spears, M.E.; Park, S.J.; Youkana, D.; Doshi, M.B.; Peppers, A.; Li, R.; Joseph, A.B.; et al. Selenium Detoxification Is Required for Cancer-Cell Survival. *Nat. Metab.* **2020**, *2*, 603–611. [[CrossRef](#)]
34. Zonaro, E.; Lampis, S.; Turner, R.J.; Qazi, S.J.S.; Vallini, G. Biogenic Selenium and Tellurium Nanoparticles Synthesized by Environmental Microbial Isolates Efficaciously Inhibit Bacterial Planktonic Cultures and Biofilms. *Front. Microbiol.* **2015**, *6*, 584. [[CrossRef](#)] [[PubMed](#)]
35. Wang, T.; Yang, L.; Zhang, B.; Liu, J. Extracellular Biosynthesis and Transformation of Selenium Nanoparticles and Application in H₂O₂ Biosensor. *Colloids Surf. B Biointerfaces* **2010**, *80*, 94–102. [[CrossRef](#)] [[PubMed](#)]
36. Jeong, U.; Xia, Y. Synthesis and Crystallization of Monodisperse Spherical Colloids of Amorphous Selenium. *Adv. Mater.* **2005**, *17*, 102–106. [[CrossRef](#)]

37. Upende, G.; Bharadwaj, S.; Awasthi, A.M.; Chandra Mouli, V. Glass Transition Temperature-Structural Studies of Tungstate Tellurite Glasses. *Mater. Chem. Phys.* **2009**, *118*, 298–302. [[CrossRef](#)]
38. Espinosa-Ortiz, E.J.; Rene, E.R.; Guyot, F.; van Hullebusch, E.D.; Lens, P.N.L. Biomineralization of Tellurium and Selenium-Tellurium Nanoparticles by the White-Rot Fungus *Phanerochaete chrysosporium*. *Int. Biodeterior. Biodegrad.* **2017**, *124*, 258–266. [[CrossRef](#)]
39. Zhang, W.; Chen, Z.; Liu, H.; Zhang, L.; Gao, P.; Li, D. Biosynthesis and Structural Characteristics of Selenium Nanoparticles by *Pseudomonas alcaliphila*. *Colloids Surf. B Biointerfaces* **2011**, *88*, 196–201. [[CrossRef](#)] [[PubMed](#)]
40. Gates, B.; Mayers, B.; Cattle, B.; Xia, Y. Synthesis and Characterization of Uniform Nanowires of Trigonal Selenium. *Adv. Funct. Mater.* **2002**, *12*, 219–227. [[CrossRef](#)]
41. Li, C.; Gao, F.; Wang, Y.; Zhao, L.; Li, H.; Jiang, Y. Advances of Bioactive Tellurium Nanomaterials in Anti-Cancer Phototherapy. *Mater. Adv.* **2022**, *3*, 6397–6414. [[CrossRef](#)]
42. Borghese, R.; Baccolini, C.; Francia, F.; Sabatino, P.; Turner, R.J.; Zannoni, D. Reduction of Chalcogen Oxyanions and Generation of Nanoprecipitates by the Photosynthetic Bacterium *Rhodobacter Capsulatus*. *J. Hazard. Mater.* **2014**, *269*, 24–30. [[CrossRef](#)]
43. Klonowska, A.; Heulin, T.; Vermeglio, A. Selenite and Tellurite Reduction by *Shewanella Oneidensis*. *Appl. Environ. Microbiol.* **2005**, *71*, 5607–5609. [[CrossRef](#)]
44. Turner, R.J.; Weiner, J.H.; Taylor, D.E. The Tellurite-Resistance Determinants *tehA* and *klaA* Have Different Biochemical Requirements. *Microbiology* **1995**, *141*, 3133–3140. [[CrossRef](#)] [[PubMed](#)]
45. Fernández-Llamosas, H.; Castro, L.; Blázquez, M.L.; Díaz, E.; Carmona, M. Biosynthesis of Selenium Nanoparticles by *Azoarcus* sp. CIB. *Microb. Cell Factories* **2016**, *15*, 109. [[CrossRef](#)] [[PubMed](#)]
46. Ni, T.W.; Staicu, L.C.; Nemeth, R.S.; Schwartz, C.L.; Crawford, D.; Seligman, J.D.; Hunter, W.J.; Pilon-Smits, E.A.H.; Ackerson, C.J. Progress toward Clonable Inorganic Nanoparticles. *Nanoscale* **2015**, *7*, 17320–17327. [[CrossRef](#)] [[PubMed](#)]
47. Kessi, J.; Hanselmann, K.W. Similarities between the Abiotic Reduction of Selenite with Glutathione and the Dissimilatory Reaction Mediated by *Rhodospirillum rubrum* and *Escherichia coli*. *J. Biol. Chem.* **2004**, *279*, 50662–50669. [[CrossRef](#)] [[PubMed](#)]
48. Wang, Y.; Shu, X.; Zhou, Q.; Fan, T.; Wang, T.; Chen, X.; Li, M.; Ma, Y.; Ni, J.; Hou, J.; et al. Selenite Reduction and the Biogenesis of Selenium Nanoparticles by *Alcaligenes Faecalis* Se03 Isolated from the Gut of *Monoctonus alternatus* (Coleoptera: Cerambycidae). *Int. J. Mol. Sci.* **2018**, *19*, 2799. [[CrossRef](#)] [[PubMed](#)]
49. Song, D.; Li, X.; Cheng, Y.; Xiao, X.; Lu, Z.; Wang, Y.; Wang, F. Aerobic Biogenesis of Selenium Nanoparticles by *Enterobacter Cloacae* Z0206 as a Consequence of Fumarate Reductase Mediated Selenite Reduction. *Sci. Rep.* **2017**, *7*, 3239. [[CrossRef](#)] [[PubMed](#)]
50. Li, D.-B.; Cheng, Y.-Y.; Wu, C.; Li, W.-W.; Li, N.; Yang, Z.-C.; Tong, Z.-H.; Yu, H.-Q. Selenite Reduction by *Shewanella oneidensis* MR-1 Is Mediated by Fumarate Reductase in Periplasm. *Sci. Rep.* **2014**, *4*, 3735. [[CrossRef](#)] [[PubMed](#)]
51. Painter, E.P. The Chemistry and Toxicity of Selenium Compounds, with Special Reference to the Selenium Problem. *Chem. Rev.* **1941**, *28*, 179–213. [[CrossRef](#)]
52. Avazéri, C.; Turner, R.J.; Pommier, J.; Weiner, J.H.; Giordano, G.; Verméglio, A. Tellurite Reductase Activity of Nitrate Reductase Is Responsible for the Basal Resistance of *Escherichia coli* to Tellurite. *Microbiology* **1997**, *143*, 1181–1189. [[CrossRef](#)]
53. Basaglia, M.; Toffanin, A.; Baldan, E.; Bottegali, M.; Shapleigh, J.P.; Casella, S. Selenite-Reducing Capacity of the Copper-Containing Nitrite Reductase of *Rhizobium sullae*. *FEMS Microbiol. Lett.* **2007**, *269*, 124–130. [[CrossRef](#)]
54. DeMoll-Decker, H.; Macy, J.M. The Periplasmic Nitrite Reductase of *Thauera Selenatis* May Catalyze the Reduction of Selenite to Elemental Selenium. *Arch. Microbiol.* **1993**, *160*, 241–247. [[CrossRef](#)]
55. Taylor, D.E. Bacterial Tellurite Resistance. *Trends Microbiol.* **1999**, *7*, 111–115. [[CrossRef](#)] [[PubMed](#)]
56. Wells, M.; McGarry, J.; Gaye, M.M.; Basu, P.; Oremland, R.S.; Stolz, J.F. Respiratory Selenite Reductase from *Bacillus selenitireducens* Strain MLS10. *J. Bacteriol.* **2019**, *201*, e00614-18. [[CrossRef](#)] [[PubMed](#)]
57. Nancharaiah, Y.V.; Lens, P.N.L. Selenium Biomineralization for Biotechnological Applications. *Trends Biotechnol.* **2015**, *33*, 323–330. [[CrossRef](#)] [[PubMed](#)]
58. Debieux, C.M.; Dridge, E.J.; Mueller, C.M.; Splatt, P.; Paszkiewicz, K.; Knight, I.; Florance, H.; Love, J.; Titball, R.W.; Lewis, R.J.; et al. A Bacterial Process for Selenium Nanosphere Assembly. *Proc. Natl. Acad. Sci. USA* **2011**, *108*, 13480–13485. [[CrossRef](#)] [[PubMed](#)]
59. Nancharaiah, Y.V.; Lens, P.N.L. Ecology and Biotechnology of Selenium-Respiring Bacteria. *Microbiol. Mol. Biol. Rev.* **2015**, *79*, 61–80. [[CrossRef](#)] [[PubMed](#)]
60. Fischer, S.; Krause, T.; Lederer, F.; Merroun, M.L.; Shevchenko, A.; Hübner, R.; Firkala, T.; Stumpf, T.; Jordan, N.; Jain, R. *Bacillus safensis* JG-B5T Affects the Fate of Selenium by Extracellular Production of Colloidally Less Stable Selenium Nanoparticles. *J. Hazard. Mater.* **2020**, *384*, 121146. [[CrossRef](#)]
61. Sintubin, L.; De Windt, W.; Dick, J.; Mast, J.; van der Ha, D.; Verstraete, W.; Boon, N. Lactic Acid Bacteria as Reducing and Capping Agent for the Fast and Efficient Production of Silver Nanoparticles. *Appl. Microbiol. Biotechnol.* **2009**, *84*, 741–749. [[CrossRef](#)]
62. Zambonino, M.C.; Quizhpe, E.M.; Jaramillo, F.E.; Rahman, A.; Santiago Vispo, N.; Jeffryes, C.; Dahoumane, S.A. Green Synthesis of Selenium and Tellurium Nanoparticles: Current Trends, Biological Properties and Biomedical Applications. *Int. J. Mol. Sci.* **2021**, *22*, 989. [[CrossRef](#)]

Disclaimer/Publisher’s Note: The statements, opinions and data contained in all publications are solely those of the individual author(s) and contributor(s) and not of MDPI and/or the editor(s). MDPI and/or the editor(s) disclaim responsibility for any injury to people or property resulting from any ideas, methods, instructions or products referred to in the content.